

Recent developments in numerical homogenization

Daniela P. Boso

*Department of Structural and Transportation Engineering
University of Padua, Via Marzolo 9, 35131 Padua, Italy
e-mail: boso@dic.unipd.it*

Marek Lefik

*Chair of Geotechnical Engineering and Engineering Structures
Technical University of Łódź, Al. Politechniki 6, 93-590 Łódź, Poland
e-mail: marek.lefik@p.lodz.pl*

Bernhard A. Schrefler

*Department of Structural and Transportation Engineering
University of Padua, Via Marzolo 9, 35131 Padua, Italy
e-mail: bas@dic.unipd.it*

(Received in the final form February 11, 2010)

This paper deals with homogenization of non linear fibre-reinforced composites in the coupled thermo-mechanical field. For this kind of structures, i.e. inclusions randomly dispersed in a matrix, the self consistent methods are particularly suitable to describe the problem. Usually, in the framework of the self consistent scheme the homogenized material behaviour is obtained with a symbolic approach. For the non linear case, that method may become tedious. This paper presents a different, fully numerical procedure. The effective properties are determined by minimizing a functional expressing the difference (in some chosen norm) between the solution of the heterogeneous problem and the equivalent homogenous one. The heterogeneous problem is solved with the Finite Element method, while the second one has its analytical solution. The two solutions are written as a function of the (unknown) effective parameters, so that the final global solution is found by iterating between the two single solutions. Further, it is shown that the considered homogenization scheme can be seen as an inverse problem and Artificial Neural Networks are used to solve it.

Keywords: Generalized Self-Consistent-Like method, non-linear homogenization, Artificial Neural Networks, inverse problems, thermo-mechanical analysis, multiscale modelling, unsmearing

1. INTRODUCTION

Composite materials are commonly applied in engineering practice. They allow to take advantage of the different properties of the component materials, of the geometric structure and of the interaction between the constituents to obtain a tailored behaviour as a final result.

Composite materials are usually multiscale in nature, i.e. the scale of the constituents is of lower order than the scale of the resulting material and structure. To fix the ideas, we speak of *macroscopic scale* as the particular scale in which we are interested in (e.g. at structural level) while the lower scales are referred to as *microscopic scales* (sometimes an intermediate scale is called *mesoscopic scale*). We exclude here scales at atomic level, which would require a separate study.

For most of the analyses of composite structures *effective* or *homogenized* material properties are used, instead of taking into account the individual component properties and their geometrical arrangements. A lot of effort went into the development of mathematical and numerical models

to derive homogenized material properties directly from those of the constituents and from their microstructure. Many engineering problems are solved at macroscopic scale with such homogenized properties. However, in many instances such analyses are not accurate enough.

In principle it would be possible to refer directly to the microscopic scale, but such microscopic models are often far too complex to handle for the analysis of a large structure. Further, the obtained data would be often redundant and complicated procedures would be required to extract information of interest.

A way out is what is now commonly known as *multiscale modelling*, where macroscopic and microscopic models are coupled to take advantage of the efficiency of macroscopic models and the accuracy of the microscopic ones. The scope of such multiscale modelling is to design combined macroscopic-microscopic computational methods that are more efficient than solving the full microscopic model and at the same time give the information that we need to the desired accuracy [1].

In the case of material and structural multiscale modelling and in homogenization in general, one usually proceeds from the lower scales upward in order to obtain equivalent material properties. However, it is also important to be able to step down through the scales until the desired scale of the real, not homogenized, material is reached. This technique is often known as *unsmearing, localization or recovering method*. Usually in a global analysis both aspects need to be pursued, think for instance of a damage or fracture analysis. The procedure may be either of a *serial coupling*, which represents some sort of data passing up and down the scales, or *concurrent coupling* where both microscale and macroscale models are strongly interwoven and have to be addressed continuously as the computation goes on. This last case is particularly the case in non linear situations.

In this paper both linear and non-linear material behaviours are considered. The case of non linear composites with random microstructure is dealt with in detail. In Section 2 a brief distinction for linear and non linear cases is outlined and in Section 3 we describe our recent developments of the self-consistent methods for elastic-plastic and brittle materials in the coupled thermo-mechanical field. In Section 4 numerical examples of this method are reported. Concluding remarks close the paper in Section 5.

2. LINEAR AND NON-LINEAR BEHAVIOUR

Over the last decades a large body of literature was developed, which deals with the micromechanical modelling techniques for heterogeneous materials. As far as the effective properties are concerned, the various approaches may be divided into two main categories, depending upon the microstructure characteristics.

In case of composites with linear constitutive behaviour, if the microstructure is sufficiently regular to be considered periodic, the effective properties may be determined in terms of unit cell problems with appropriate boundary conditions [2, 3]. If the microstructure is not regular the effective properties cannot be determined exactly. Thus the goal consists instead in the definition of the range of the possible effective behaviour in terms of bounds, which depend on some parameters characterizing the microstructure, such as for instance the volume ratio of the inclusions in a matrix. To this purpose many homogenisation methods have been developed. We mention the pioneering studies by Voigt [4] and Reuss [5], who formulated rigorous bounds for the effective moduli of composites with prescribed volume fraction. One can interpret the Voigt and Reuss fields as providing two microfields extremes, since the Voigt stress field is one where the tractions at the phase boundaries cannot be in equilibrium, that is, statically inadmissible, while the implied Reuss strains are such that the heterogeneities and the matrix could not be perfectly bonded, that is, kinematically inadmissible.

Some decades later Hashin and Shtrikman [6–8] presented an extension of the method, based on variational formulations. If the microstructure is composed of a matrix and spheric or spheroidal inclusions, the effective behaviour of composite can be obtained by means of the self-consistent method [9–13].

If the composite materials have non linear constitutive behaviour, for periodic microstructure the effective properties can still be obtained in terms of unit cell problems with appropriate boundary conditions [14–19]. For composites with random microstructures the first bounds are obtained by Bishop and Hill [20, 21] for rigid perfectly plastic polycrystals.

In the framework of non linear bounds we mention also the work by Willis [22] and Talbot [23], which provides extensions of the Hashin-Shtrikman variational principles for non linear composites. Their work is followed by the introduction of several new variational principles making use of appropriately chosen “linear comparison composites”, which allow the determination of Hashin-Shtrikman and more general bounds and estimates, directly from corresponding estimates for linear composites. These include the variational principles of Ponte Castañeda [24, 25] and Talbot and Willis [26] for general classes of nonlinear composites, of Suquet [27] for power-law composites and Olson [28] for perfectly plastic composites.

3. THE SELF-CONSISTENT METHOD AND ITS DEVELOPMENT

3.1. A brief historical overview

Considering a composite made of particles dispersed in a matrix, one can assume that there is no particle interaction, so that the problem is transformed into the analysis of a single inclusion immersed in an infinite domain made of the matrix material [29]. However, the assumption of non-interacting particles can lead to unreliable results, especially for randomly dispersed particulate microstructure.

An improvement of this approach is given by the *Self-Consistent* (SC) method [10, 12]. The main idea is still to replace the problem of the interaction among many particles by the problem of interaction of one particle and an infinite matrix: but now the unbounded domain is made of the effective medium. Unfortunately, the self-consistent method can produce negative effective bulk and shear responses, for voids, for volume fractions of 50% and higher. For rigid inclusions, it produces infinite effective bulk responses for any volume fraction and infinite effective shear responses above 40% [30, 31].

To avoid this problem, the *Generalized Self-Consistent* (GSC) methods encase the particle in a shell of matrix material, surrounded by the effective medium (see e.g. [32]). However, such methods also exhibit problems, which are discussed in Hashin [33].

Some extensions of the self-consistent methods for the non-linear case can be found in Hill [34], Hutchinson [35] and Berveiller and Zaoui [36].

3.2. The Generalized Self-Consistent-Like method

Usually, GSC method results with closed type formulae for the effective mechanical characteristics, obtained via some symbolic manipulations. However, in the case of thermo-elastic-plastic behaviour of components that method may become tedious. Recently we have developed a different, fully numerical approach which is suitable for homogenization of non-linear composites formed by a matrix and long fibrous inclusions: the *Generalized Self-Consistent-Like* (GSCL) method [37–39]. We take into account a continuum phase and a set of isolated long inclusions randomly distributed inside the matrix, but having the longitudinal direction parallel one to another or twisted with relatively long twist pitches. The matrix can be non linear, and inclusions can be non linear, brittle, and non homogeneous, i.e. they can have their own microstructure, composed of concentric layers of different materials. With respect to GSC method, three main points have to be evidenced:

- in the GSCL method we are not limited by the necessity of considering only a matrix where homogeneous inclusions are embedded. In our formulation an “unlimited” number of concentric cylinders can be taken into consideration, so that heterogeneous inclusions can be modelled. In the following the formulation is developed for I materials,

- this method is formulated for the coupled thermo-mechanical field,
- all material characteristics can be non linear and dependent on a certain field (e.g. temperature).

In this paper only material non linearity expressed by elastic-plastic constitutive law is taken into consideration, but we think that this approach could be easily generalized to other kinds of material non linearity.

Concerning fibre breakage, it is assumed to appear at a certain step of the loading path, without taking into account the critical energy or other critical values causing the appearance of the cracks. This method aims at identifying the effective material properties of the already damaged material, rather than giving a realistic cracking model. On the other hand, the simplest and widely used method of including the damage into a model of the thermo-mechanical behaviour of solids is based on a so called *damage parameter* [40–42]. This parameter is usually a scalar multiplier affecting the material stiffness tensor. It is rarely measured [43], usually it results from some theoretical reasoning or a priori assumptions on the constitutive behaviour. We propose a significantly different method, where we compute the effective material parameters of the damaged composite, so that a full constitutive stiffness matrix is obtained at various stages of the loading path.

GSCL homogenization inherits the most important conceptual principles from the self-consistent scheme. The heterogeneous medium is replaced by concentric cylinders made of the components of the composite. These cylinders preserve the volume fractions of the initial materials. They are immersed in the external, infinite homogeneous body endowed with the effective parameters to be identified. The solution of the heterogeneous problem surrounded by the infinite elastic body and subject to some loads is compared with the one, obtained for a homogeneous infinite body, made of the homogenized material. The effective parameters are present directly in the second solution and indirectly in the first one (as a measure of compliance of the boundary conditions). They are identified from this comparison.

3.3. Formulation of the problem

To define the GSCL method we formulate three different problems, called P1, P2 and P3.

The first one (P1) is a thermo-elastic-plastic problem defined on a composite domain (Ω_{self} in Fig. 1), taking into account temperature-dependent material characteristics. The domain is composed of $I - 1$ concentric cylinders made of different homogeneous isotropic materials (materials from 1 to $I - 2$ correspond to the heterogeneous fibrous inclusions, material $I - 1$ is the matrix) embedded in the outer infinite effective material numbered I (Fig. 2). The number of cylinders is arbitrary, but generally in a real problem it is a small value, usually there are at most three or four different starting materials.

The second one (P2) is a “thermo-elastic like” problem, formulated over an infinite, homogeneous domain (Ω_{hom} in Fig. 1). We do not make any a priori assumption on the behaviour of the effective material. P2 solution is easily found, but it has to be updated step by step, i.e. it is “path dependent” as described later.

The last problem (P3) is a minimization problem: it minimizes a suitable functional expressed as a function of the difference between the solutions of P1 and P2. In this way the homogenized material parameters are found.

Given the geometrical layout we are taking into consideration (axial symmetry), we will refer to a cylindrical coordinate system (radial coordinate r , angular coordinate Θ , and longitudinal coordinate z). Concerning the effective constitutive law, because of the symmetry we can suppose that the homogenized material is isotropic in the plane (r, Θ) while the mechanical and thermal properties may result different along the longitudinal direction z .

We also suppose that the cross section (in the plane (r, Θ)) remains plane. We impose the condition of continuity of displacements and stresses on each interface and the vanishing of the stress field for infinite r .

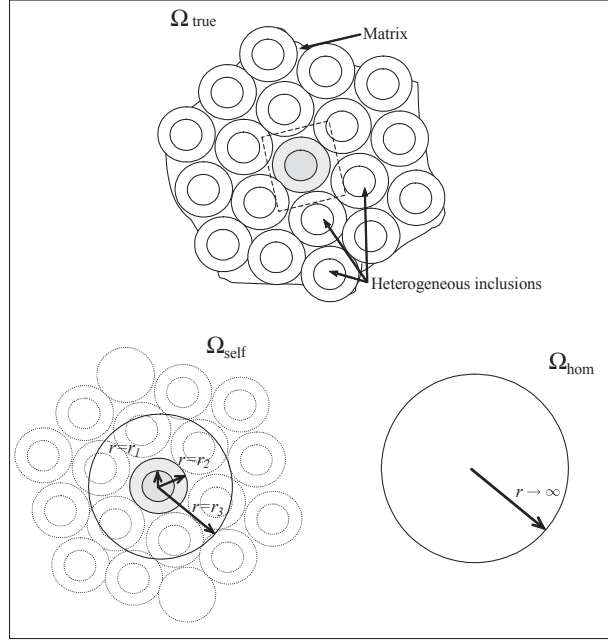


Fig. 1. Composite material made of a matrix and heterogeneous inclusions (Ω_{true} in upper image), schematization for the GSCL formulation (Ω_{self} in bottom left image) and the equivalent homogenized domain (Ω_{hom} in bottom right image). The radii of Ω_{self} are computed taking into consideration the phase volume ratio

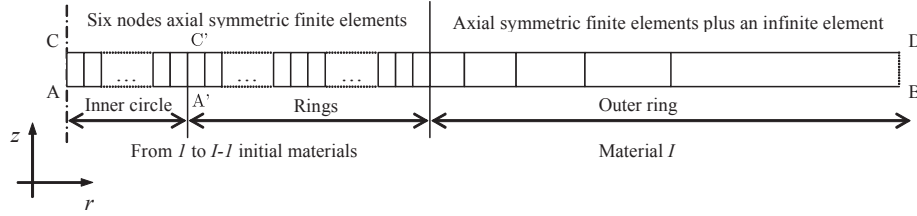


Fig. 2. Cross-section of the domain Ω_{self} in the plane (r, z) and scheme of the FE discretization

In this work we take into consideration a thermal load, to better evaluate the coupling between the thermal and mechanical field.

Problem P1

The above considerations allow us to write the following constitutive relations for any homogeneous cylinder i and for the external infinite effective medium I ((1a) and (1b), respectively):

$$\begin{bmatrix} \varepsilon_r^{\text{el } i} \\ \varepsilon_\theta^{\text{el } i} \\ \varepsilon_z^{\text{el } i} \end{bmatrix} = \frac{1}{E^i} \begin{bmatrix} 1 & -\nu^i & -\nu^i \\ -\nu^i & 1 & -\nu^i \\ -\nu^i & -\nu^i & 1 \end{bmatrix} \begin{bmatrix} \sigma_r^i \\ \sigma_\theta^i \\ \sigma_z^i \end{bmatrix} + \beta^i \Delta T, \quad i \in (1, \dots, I-1), \quad (1a)$$

$$\begin{bmatrix} \varepsilon_r^I \\ \varepsilon_\theta^I \\ \varepsilon_z^I \end{bmatrix} = \begin{bmatrix} \frac{1}{E} & -\frac{\nu}{E} & -\frac{\nu_z}{E_z} \\ -\frac{\nu}{E} & \frac{1}{E} & -\frac{\nu_z}{E_z} \\ -\frac{\nu_z}{E_z} & -\frac{\nu_z}{E_z} & \frac{1}{E_z} \end{bmatrix} \begin{bmatrix} \sigma_r^I \\ \sigma_\theta^I \\ \sigma_z^I \end{bmatrix} + \Delta T \begin{bmatrix} \beta \\ \beta \\ \beta_z \end{bmatrix}, \quad (1b)$$

where the superscript i is related to the given initial i -th material of the composite domain (Fig. 1) and the material properties without superscript are related to the fictitious, homogenized body

(material I), E is the Young modulus, ν is the Poisson's coefficient and β is the thermal expansion coefficient. Superscript el stands for elastic. The other symbols have the usual meaning: ε_j is the j -th component of strain, σ_j is the j -th component of stress and T is temperature. We point out that in Eqs. (1a) all material characteristics are known, while in equations Eqs. (1b) they are unknown (they will be identified by the minimization process of problem P3). As mentioned, the effective material behaviour may be non-linear and non-elastic (see below), the behaviour (1b) is identified as a global behaviour calculated step by step, so that the dependence on the load path is taken into consideration "automatically" because of the solution process adopted.

The displacement field \mathbf{u} is related to the strain field by the usual equations (small displacements and small strains are assumed):

$$\varepsilon_r^i = \frac{\partial u_r^i(r)}{\partial r}, \quad \varepsilon_\theta^i = \frac{u_r^i(r)}{r}, \quad \varepsilon_z^i = \frac{\partial u_z^i(z)}{\partial z}, \quad i \in (1, \dots, I). \quad (2)$$

In each sub-domain the equilibrium equations written in cylindrical coordinates are:

$$\frac{\partial \sigma_r^i}{\partial r} + \frac{\sigma_r^i - \sigma_\theta^i}{r} = 0, \quad \frac{\partial \sigma_z^i}{\partial z} = 0, \quad i \in (1, \dots, I). \quad (3)$$

Finally, the conditions of continuity of stress and displacements at the interfaces can be written as:

$$|u^i = u^{i+1}|_{r=r_i}, \quad |\sigma_r^i(u_r^i) = \sigma_r^{i+1}(u_r^{i+1})|_{r=r_i}, \quad \sigma_r^I(u_r^I)|_{r \rightarrow \infty} = 0, \quad i \in (1, \dots, I-1). \quad (4)$$

If the initial materials are elastic-plastic, the set of Eqs. (1) to (4) is completed by the formulation of the plastic behaviour.

We consider here classical rate-independent plasticity within the context of the three dimensional infinitesimal theory. We assume the additive decomposition of total strain tensor $\varepsilon^i = \varepsilon^{\text{el}i} + \varepsilon^{\text{pl}i} + \varepsilon^{\text{T}i}$, where $\varepsilon^{\text{T}i} = \beta^i \Delta T$ is the thermal strain) and postulate the usual elastic stress-strain relation $\boldsymbol{\sigma}^i = \mathbf{C}^i (\boldsymbol{\varepsilon}^i - \boldsymbol{\varepsilon}^{\text{pl}i} - \boldsymbol{\varepsilon}^{\text{T}i})$, where \mathbf{C}^i is the tensor of elastic moduli for i -th material. The admissible states in stress space are defined by:

$$f^i(\boldsymbol{\sigma}^i, \mathbf{q}^i) \leq 0, \quad (5)$$

where \mathbf{q}^i is a suitable set of internal variables for i -th material. The flow rule and hardening law can be written as (associative plasticity):

$$\dot{\boldsymbol{\varepsilon}}^{\text{pl}i} = \lambda^i \frac{\partial f^i}{\partial \boldsymbol{\sigma}^i}, \quad (6)$$

$$\dot{\mathbf{q}}^{\text{pl}i} = -\lambda^i \mathbf{D} \frac{\partial f^i}{\partial \mathbf{q}^i}, \quad (7)$$

where \mathbf{D} stands for the matrix of generalized plastic moduli of the i -th sub-domain and λ^i is the consistency parameter, which is assumed to obey the Kuhn-Tucker complementarity conditions:

$$\lambda_i \geq 0, \quad f^i(\boldsymbol{\sigma}, \mathbf{q}) \leq 0, \quad \lambda^i f^i(\boldsymbol{\sigma}, \mathbf{q}) = 0. \quad (8)$$

In addition to conditions (8), λ^i satisfies the consistency requirement $\lambda^i \dot{f}^i(\boldsymbol{\sigma}, \mathbf{q}) = 0$.

At each step we have to check if the stress tensor lies inside the yield surface. If the stress tensor violates condition (5), the well know return-mapping procedure [44, 45] is used to calculate the correct strain field. In this paper the Huber-Hencky-von Mises yield surface with isotropic hardening has been used, but any other yield surface can be applied in this numerical approach.

The problem P1 is composed of the set of Eqs. (1) to (7) and can be formulated as follows:

Find a triplet $\{\boldsymbol{\sigma}, \boldsymbol{\varepsilon}, \mathbf{u}\}$ formed by two tensor fields and a vector field defined over the domain Ω_{self} (Fig. 1), such that for each given, uniform and monotonic increment ΔT of temperature T they satisfy Eqs. (1) to (7) and:

$$\lambda_i \geq 0, \quad f^i(\boldsymbol{\sigma}, \mathbf{q}) \leq 0, \quad \lambda^i f^i(\boldsymbol{\sigma}, \mathbf{q}) = 0.$$

In the following the solution of the problem P1 is called $\{\boldsymbol{\sigma}_{\text{P1}}, \boldsymbol{\varepsilon}_{\text{P1}}, \mathbf{u}_{\text{P1}}\}$. The analytical solution of P1 exists in the thermo-elastic case [46], while for the non linear case it is not so easy to find a closed form solution. In this paper we prefer to replace the exact solution of P1 by its finite element approximation. This allows for a more general approach, we can take into consideration material characteristics depending upon temperature in a simple way, and cycling loads can be applied. The FE model required is really small and easy (Fig. 2), so that the numerical solutions is obtained rapidly.

Problem P2

Let us define the usual set of partial differential equations of thermo-elasticity defined over a homogeneous infinite domain (Ω_{hom} in Fig. 1) having the same (unknown) material properties like the outer, infinite sub-domain of problem 1. The constitutive equations inside the infinite domain are given by:

$$\begin{bmatrix} \varepsilon_r \\ \varepsilon_\theta \\ \varepsilon_z \end{bmatrix} = \begin{bmatrix} \frac{1}{E} & -\frac{\nu}{E} & -\frac{\nu_z}{E_z} \\ -\frac{\nu}{E} & \frac{1}{E} & -\frac{\nu_z}{E_z} \\ -\frac{\nu_z}{E_z} & -\frac{\nu_z}{E_z} & \frac{1}{E_z} \end{bmatrix} \begin{bmatrix} \sigma_r \\ \sigma_\theta \\ \sigma_z \end{bmatrix} + \Delta T \begin{bmatrix} \beta \\ \beta \\ \beta_z \end{bmatrix}. \quad (9)$$

The consistency and equilibrium equations are given by

$$\varepsilon_r = \frac{\partial u_r(r)}{\partial r}, \quad \varepsilon_\theta = \frac{u_r(r)}{r}, \quad \varepsilon_z = \frac{\partial u_z(z)}{\partial z}, \quad (10)$$

$$\frac{\partial \sigma_r}{\partial r} + \frac{\sigma_r - \sigma_\theta}{r} = 0, \quad \frac{\partial \sigma_z}{\partial z} = 0. \quad (11)$$

The problem P2 can be formulated as:

Find a triplet $\{\boldsymbol{\sigma}, \boldsymbol{\varepsilon}, \mathbf{u}\}$ formed by two tensor fields and a vector field defined over the domain Ω_{hom} (Fig. 1) such that for each given, uniform and monotonic increment ΔT of temperature T they satisfy Eqs. (9) to (11) and:

$$\sigma_r(u_r)|_{r \rightarrow \infty} = 0.$$

The solution of the problem P2 is easily obtained in closed form. The displacement and stress field are given by:

$$u_r = r((\beta + \nu_z \beta_z) \Delta T - \nu_z \varepsilon_z), \quad (12)$$

$$\sigma_r = \sigma_\theta = 0, \quad \sigma_z = (\varepsilon_z - \beta_z \Delta T) E_z \quad (13)$$

and this solution is called $\{\boldsymbol{\sigma}_{\text{P2}}, \boldsymbol{\varepsilon}_{\text{P2}}, \mathbf{u}_{\text{P2}}\}$ in the following. Intentionally we do not take into consideration a possible yielding of the effective material, because it would be less clear, first of all from a conceptual point of view but also from a computational one. Instead, we will work with many elastic P2 problems, with different elastic parameters at each step of the solution and at each level of load.

Problem P3

In the two previous problems it is clear that both $\{\boldsymbol{\sigma}_{P1}, \boldsymbol{\varepsilon}_{P1}, \mathbf{u}_{P1}\}$ and $\{\boldsymbol{\sigma}_{P2}, \boldsymbol{\varepsilon}_{P2}, \mathbf{u}_{P2}\}$ are parameterised by the set $\{E, \nu, E_z, \nu_z, \beta, \beta_z\}$: the first one because of the presence of the outer region I , the second one directly.

We can define now the essential problem of the GSCL homogenization:

Find an ordered set of parameters $\{E, \nu, E_z, \nu_z, \beta, \beta_z\}$ defined over the infinite domain Ω_{hom} (Fig. 1) such that for each given, uniform and monotonic increment ΔT of temperature T a given norm of the distance between the solutions of problems P1 and P2:

$$F_{12} = \|f((\boldsymbol{\sigma}_{P1} - \boldsymbol{\sigma}_{P2}), (\boldsymbol{\varepsilon}_{P1} - \boldsymbol{\varepsilon}_{P2}), (\mathbf{u}_{P1} - \mathbf{u}_{P2}))\|.$$

attains its minimum.

The values of the material characteristics minimising the given norm F_{12} according to the GSCL approach are called $E^h = \{E^h, \nu^h, E_z^h, \nu_z^h, \beta^h, \beta_z^h\}$ (*effective or homogenised properties*):

$$E^h = \{E^h, \nu^h, E_z^h, \nu_z^h, \beta^h, \beta_z^h\} = \min_{\{E, \nu, E_z, \nu_z, \beta, \beta_z\}} F_{12}(E, \nu, E_z, \nu_z, \beta, \beta_z) \quad (14)$$

Different forms for the norm F_{12} can be chosen. We observe that if the following norm F_{12H} :

$$F_{12H} = \left(\int_{\Omega_{\text{hom}}} \boldsymbol{\varepsilon}_{P2} : \boldsymbol{\sigma}_{P2} d\Omega_{\text{hom}} - \left(\int_{\Omega_{\text{self}}} \boldsymbol{\varepsilon}_{P1} d\Omega_{\text{self}} \right) : \left(\int_{\Omega_{\text{self}}} \boldsymbol{\sigma}_{P1} d\Omega_{\text{self}} \right) \right)^2 \quad (15)$$

attains its minimum, the Hill postulate is verified. Therefore in the present paper we take the norm F as the suitably rewritten, commonly accepted Hill's postulate.

The minimization of the norm F_{12H} is done numerically. In the classical formulation of the self consistent method, generally the solution of the problem P1 (formulated for the mechanical field, not the thermo-mechanical one) and the results of the minimization problem P3 are found symbolically. In the GSCL method, the (thermo-mechanical) solution of P1 and P3 are found by means of numerical procedures resulting e.g. by the finite element approximation of $\{\boldsymbol{\sigma}_{P1}, \boldsymbol{\varepsilon}_{P1}, \mathbf{u}_{P1}\}$ and a set of approximated values E^h . In detail, the minimum of F_{12H} will be searched numerically among the FE solutions of the problem 1, having at hand the corresponding solution of the problem P2.

3.4. Numerical solution of the problem P1

We take into consideration a FE discretization consisting of a mesh of a certain number of elements suitable to exploit the axial symmetry of our problem. As usual by means of the shape functions, displacements are calculated in nodal position, while strain and stress fields in Gauss points. The sub-domains are discretized as follows: the inner cylinder and nearby ones (till the last but one) are modelled by a fine mesh composed of axial symmetric elements with rectangular cross section (r - z plane), with six nodes (three nodes along the edge parallel to the r direction and two nodes along the longitudinal direction z (axis of symmetry)) and two degrees of freedom per node. The infinite region of the outer cylinder is discretized with axial symmetric finite elements as before and an outer infinite element (see [47] for the description of this kind of element). In Fig. 2 a sketch of the discretization is illustrated.

Concerning the boundary conditions, along the line $CC'D$ (Fig. 2), in all nodes the displacement along z direction is set to zero. Radial displacement is set to zero along line AC . Along the edge $AA'B$ vertical displacements at each node are given and equal (plane section on (r, Θ)).

In the cracked situation, for example by supposing that the inner fibre breaks, we release the longitudinal degree of freedom of line CC' , which therefore is no more set to zero. All the other boundary conditions remain the same.

3.5. Numerical solution of the problem P3

It is clear that the dependence of the norm F_{12H} upon the set of unknown effective material parameters $\{E, \nu, E_z, \nu_z, \beta, \beta_z\}$ is non linear. Given the geometrical characteristics of our problem, it could be possible to compute the effective material parameters along the longitudinal direction (E_z and β_z) as the solution of a set of springs in parallel. However, this is strictly valid only in the elastic range. When a material starts to yield, an additional cylinder inside the previously elastic material is formed, the radius of which cannot be determined a priori. A more difficult situation arises if cracks occur. As a consequence in our computations we treat all the effective material parameters as unknowns, having at most an estimated (or real) initial value. The chosen initial values have an important influence on the velocity and even the convergence of the numerical procedure used.

To simplify the notation, the ordered set of material parameters will be denoted in the following by a single symbol p with an index varying from 1 to 6:

$$F_{12H} = F_{12H}(E, \nu, E_z, \nu_z, \beta, \beta_z) = F_{12H}(p_i), \quad i = 1, \dots, 6. \quad (16)$$

3.6. Steepest descent algorithm

We apply a gradient descent algorithm, and the initial gradient of the norm F_{12H} of the distance between the solutions of P1 and P2 is computed numerically as the initial central finite difference.

$$G_j(\tilde{p}_i) \cong \frac{1}{2dp_j} (F_{12H}(\tilde{p}_k, \tilde{p}_j + dp_j) - F_{12H}(\tilde{p}_k, \tilde{p}_j - dp_j)). \quad (17)$$

It is relatively easy to determine a convenient increment of p_j . For all effective material parameters the true value is certainly in between the corresponding maximum and minimum value of the components.

$$dp_j = \left(\max_{k=(1, \dots, I)} p_j - \min_{k=(1, \dots, I)} p_j \right) / N, \quad (18)$$

where k refers to the k -th material and N is an arbitrary large number. In our computations $N = 100$ was sufficient.

The simplest starting point of the algorithm is:

$$p_j^0 = \left(\max_{k=(1, \dots, I)} p_j + \min_{k=(1, \dots, I)} p_j \right) / 2. \quad (19)$$

As an alternative, taking the initial values for the effective Young modulus and Poisson ratio by considering Gibiansky's bounds [48] is also a good choice.

The iterative procedure of the steepest descent is defined by the following formula:

$$p_i^{t+1} = p_i^t - \eta G_i(p_j^t), \quad (20)$$

where t is the current step and starts from zero. The parameter η , which controls the rate of convergence, is estimated as the mean value of all small increments used for the numerical calculation of the gradient. To apply this scheme, it is convenient that the unit measures of the material parameters are chosen so that their numerical value have the same order of magnitude, for example they are all around 1.0.

The iteration (20) can be regarded as a kind of post processing of many FE solutions of the corresponding problem formulated for various values of $\{E, \nu, E_z, \nu_z, \beta, \beta_z\}$. Initial values of the parameters are given by Eq. (19), the values of F_{12H} are computed as a postprocessing of the FE computations for current values of parameters modified according to (17). For a complete gradient vector the FE code must be run 12 times, since we have six parameters.

The computational algorithm is presented in Table 1.

Table 1. Algorithm to solve minimization problem P3 with the steepest descent scheme

<ol style="list-style-type: none"> 1. Initialize effective properties $p^{\text{eff}} = \{E, \nu, E_z, \nu_z, \beta, \beta_z\}$ according to Eq. (19). 2. Define increments (18). 3. Compute solution of problem P2 with the current material parameter values. 4. LOOP over all elements of the effective material properties set: <ul style="list-style-type: none"> Create backward and forward point in the vicinity of the current elements of the trial effective material property set. Write automatically an input file for FEM with the current effective material properties. Solve the problem P1 using FEM and compute the norm F_{12H} in the vicinity of the given trial parameters p^{eff}. END of LOOP. 5. Compute gradient. 6. IF the norm of the computed gradient is less than tolerance store these values as final effective properties and stop iteration. <ul style="list-style-type: none"> END of JOB. 7. ELSE: compute next approximation to the effective properties p^{eff}. 8. IF the new effective properties are close enough to the former one store these values as final effective properties and stop iteration. <ul style="list-style-type: none"> END of JOB. 9. ELSE: with the new effective properties p^{eff} go to 3.

3.7. The inverse problem

As an alternative, the values of the effective parameters can be sought as the solution of an inverse problem which is solved by means of an artificial neural network (ANN). The network is trained to approximate the dependence of the gradient of the quality measure F_{12H} upon the set of *trial* effective material parameters. The corresponding direct relation consists in the dependence of the gradient of F_{12H} evaluated on the set of *real* effective parameters. Obviously, this direct relationship is also unknown, but its identification in some discrete points in the space of the possible effective parameters is easy to obtain by using the FE method.

The inverse problem associated with the GSCL method can be described as follows:

Find an ordered set of parameters $\{E, \nu, E_z, \nu_z, \beta, \beta_z\}$ defined over the outer infinite cylinder of Ω_{self} such that for each given, uniform and monotonic increment ΔT of temperature T the functional:

$$F_{\text{self}} = \left(\int_{\Omega_{\text{self}}} \varepsilon_{\text{P1}} d\Omega_{\text{self}} \right) : \left(\int_{\Omega_{\text{self}}} \sigma_{\text{P1}} d\Omega_{\text{self}} \right) \quad (21)$$

is equal to the value of the internal energy of the infinite, homogeneous domain at temperature T and for the same given, uniform and monotonic increment ΔT of temperature T :

$$F_{\text{hom}} = \int_{\Omega_{\text{hom}}} \varepsilon_{\text{P2}} : \sigma_{\text{P2}} d\Omega_{\text{hom}}. \quad (22)$$

It is easy to note that the equation:

$$F_{\text{self}} = F_{\text{hom}} \quad (23)$$

is equivalent to the well-known Hill condition, required to hold for the representative volume of the composite. Therefore the inverse problem associated with the GSCL scheme can be reformulated as follows:

Find an ordered set of parameters $\{E, \nu, E_z, \nu_z, \beta, \beta_z\}$ defined over the outer infinite cylinder of Ω_{self} such that for each given, uniform and monotonic increment ΔT of temperature T the gradient of the functional:

$$F_{12H} \equiv (F_{\text{hom}} - F_{\text{self}})^2 \quad (24)$$

is equal to zero:

$$\mathbf{G} \equiv \frac{\partial F_{12H}}{\partial E^h} = \mathbf{0}. \quad (25)$$

We underline that the inverse problem we have formulated above is not fully classical because the right hand side of the problem depends on the unknown set of material characteristics. This is a source of additional complications and further reformulations.

A soft computing approach is used to solve this minimisation problem. In this context, the most important problem consists in direct learning of the inverse relation between material characteristics and the gradient of the error measure F_{12H} . ANNs can be applied to both formulations, i.e., $F_{\text{self}} = F_{\text{hom}}$ and $\mathbf{G} = \mathbf{0}$. We will focus our attention on the second one and for this case we will adopt the ANN based procedure that we have used in a different context for parametric identification [48].

By solving the direct problem with the FE method, we can compose numerically a suitable set of gradients of F_{12H} and their corresponding effective parameters. This database is used to train the neural network, which provides the required inverse relationship when used in recall mode. Namely, an ANN is trained with the gradients of F_{12H} presented at input, and the related values of effective parameters at output. Unfortunately this relation may suffer from an usual disadvantage of inverse relations: the function can result non-bijective. A special procedure is created for this case, consisting in splitting the set of training data into subsets, on which each function which has to be approximated by the ANN is a bijection. This is performed using two different kinds of ANN:

- a *poor* one, that gives the hyperplane over the domain of the approximated function,
- an *over-fitted* one, that passes almost exactly through all data points.

We are able to split the training data base by looking at the sign of the difference between the two approximations. This simple procedure can result tedious for functions with many zeros. Fortunately, in the case of the GSCL method the problem is usually not so complex, even if non-uniqueness cannot be excluded a priori. A brief a posteriori analysis is necessary to choose the best effective properties in the case that more than one solution is found.

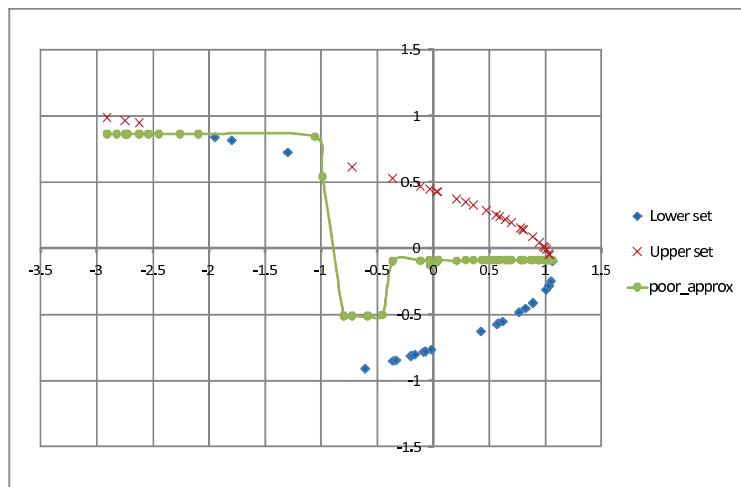
The algorithm is summarized in Table 2.

Below we illustrate the described procedure for a 1D and 2D illustrative examples. In Fig. 3 a 1D function (gradient of a third order polynomial $f(x) = (1 - x)(-0.5 - x)(-1 - x)$) is presented: the green line with circles is obtained by the poor approximation ANN used in recall mode. We compute the difference between the two results and on the basis of its sign we are able to split the values of the function into an “upper” and a “lower” subset. These subsets are analysed independently and two zeros are found, as shown in Fig. 4. In Table 3 the process of computations (training of various ANNs) is reported.

A similar illustrative example is shown in Fig. 5 and reported in Table 4. The details of the examples are described in the captions.

Table 2. Use of ANNs to look for a zero point of the gradient

<p>Current set of input patterns equal to the whole set of input patterns.</p> <ol style="list-style-type: none"> 1. For the current set of input patterns: <ol style="list-style-type: none"> a. Approximation of the gradient with an ANN, suitably chosen correctly to be able to approximate the function. <p>IF the approximation is good enough</p> <ol style="list-style-type: none"> b. Execute ANN in recall mode with $\mathbf{0}$ at input. c. Check if for the recall mode output value \mathbf{X}_0 the gradient of F is indeed $\mathbf{0}$. <p>IF yes</p> <ol style="list-style-type: none"> d. Record the output value \mathbf{X}_0 as a coordinate of the extreme of the function. e. Compute the extreme value of the function at this point (X_0), using FE model. f. Add the value of the extreme to the set of extreme values. <p>ELSE</p> <ol style="list-style-type: none"> g. Eliminate the current set of input patterns from the set of input patterns. <p>ELSE</p> <ol style="list-style-type: none"> h. Approximate the gradient with a very poor ANN. i. Check the quality of the approximation in recall mode. j. Compute signs of error. k. Split the set of input patterns into separate subsets, according to the sign of the error. <ol style="list-style-type: none"> 2. LOOP over these subsets: <ol style="list-style-type: none"> l. Take the subset of input patterns as a current set of patterns. m. Go to l. <p>END of LOOP over subsets</p> <ol style="list-style-type: none"> 3. Choose an absolute minimum within the set of recorded minima.
--

**Fig. 3.** Separation of the input patterns by a poor ANN approximation for the 1D example described in Table 3

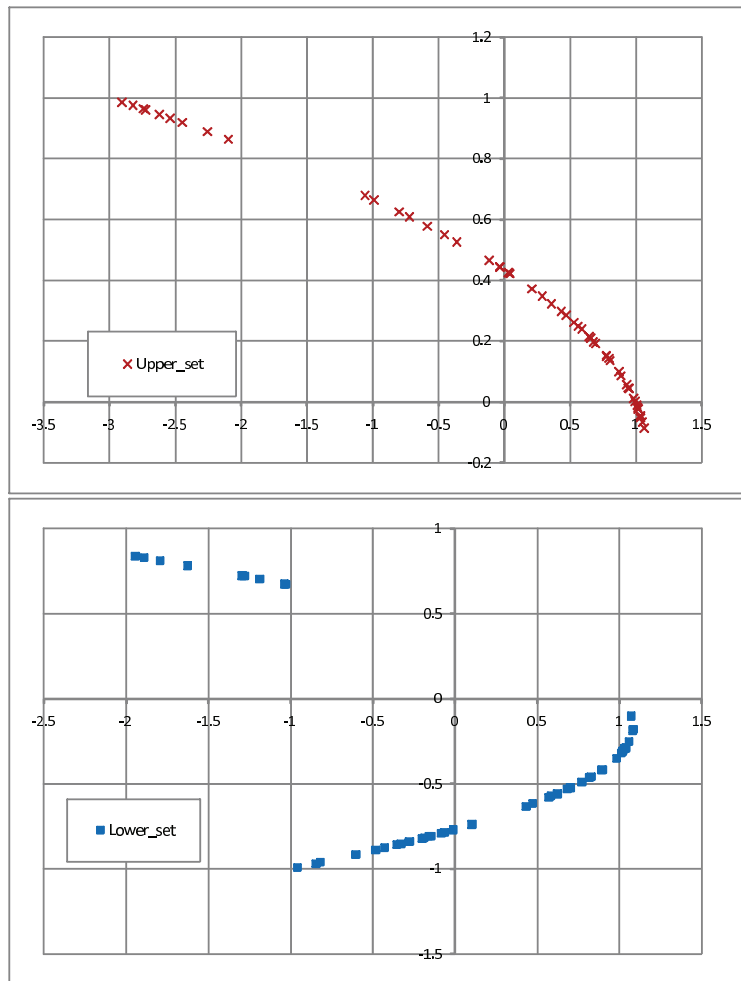


Fig. 4. Two separated subsets of the input patterns for the 1D example described in Table 3

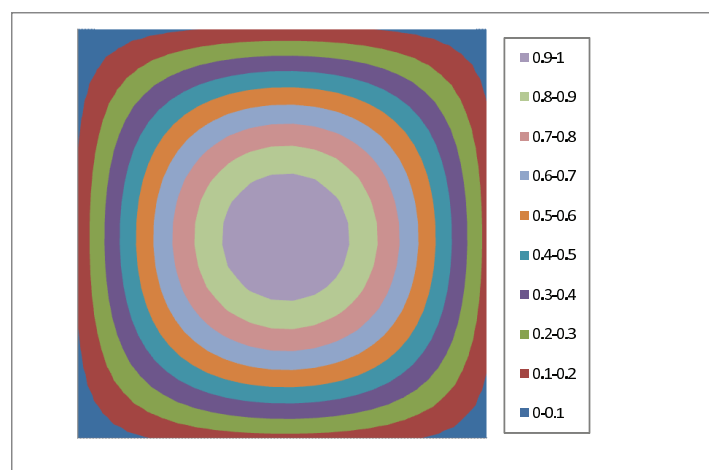


Fig. 5. Iso-lines of the function used as an illustrating example described in Table 4

Table 3. 1D case: find the minimum of the 3-rd order polynomial $f(x) = (1 - x)(-0.5 - x)(-1 - x)$

Algorithm step (Table 2)	Comments	Description of the ANN	Connections	Learning patterns/test patterns	Correlation on the learning set	Correlation on the test set
1a	Correct approximation was impossible	{2,8,8,1}	88	100/0	0.7466	—
1h	Then recall mode and splitting into two subsets of input patterns	{2,2,1}	6	100/0	0.4432	—
1a	For the “Upper_set” correct approximation achieved immediately	{2,3,2,1}	14	38/10	0.9991	0.9989
1a	For the “Lower_set” correct approximation achieved immediately	{2,3,2,1}	14	42/10	0.9987	0.9978
1b	For the “Upper_set” it gives $x_1 = 43E - 2$ (against the exact value 0.43425)	{2,3,2,1}	14	48	—	0.9871
1b	For the “Lower_set” it gives $x_2 = -76E - 2$ (against the exact value -0.7676)	{2,3,2,1}	14	52	—	0.9910
3	The minimum is at x_2					

Table 4. 2D case: find the minimum of the function: $f(x, y) = \cos x \cos y$ defined over the domain $(-1.65 < x < 1.65, -1.65 < y < 1.65)$

Algorithm step (Table 2)	Comments	Description of the ANN	Connections	Learning patterns/test patterns	Correlation on the learning set	Correlation on the test set
1a	Correct approximation was possible immediately	{2,8,8,1}	88	100/0	0.7466	—
1a again	Better approximation was defined	{3,3,2,2}	24	75/25	0.9988	0.9971
		{3,3,2,2}	24	75/25	0.9988	0.9971
1b	Recall mode, $x = 0.0$	{3,3,2,2}	24	100	—	0.9932
3	There is a single extremum (maximum)					

We point out that the training process of the artificial neural networks needed to solve the problem is quicker than the corresponding necessary FE solutions for one case of loading: from three to ten times. From the presented examples and the tests performed, we can conclude that these operations are surprisingly fast.

On the other hand, as already mentioned, usually the finite element discretization required is very simple. The simplicity of the geometry helps us to construct a very fast FE code, with a fixed, optimized mesh. For this reason, if one wants to solve the minimization problem without making use of artificial intelligence techniques, we can say that in this framework also the steepest descent algorithm works well.

4. NUMERICAL EXAMPLES

We take into consideration a real case of a superconducting strand, relevant for the international thermonuclear experimental reactor (ITER), which is now under construction.

Most of ITER coils will be made of Nb_3Sn based strands. This intermetallic compound exhibits a dependence of its superconducting properties on the strain state. Therefore the computation of the strain field is a crucial point for a good prediction of the operational conditions of the conductor [49–51]. Generally, Nb_3Sn is formed in fine filaments, which are gathered into groups and embedded in a normal metal matrix (usually bronze). A very low resistivity material, typically oxygen-free electronic (OFE) copper, usually surrounds the area of filaments, and is separated from them by a barrier (Fig. 6).

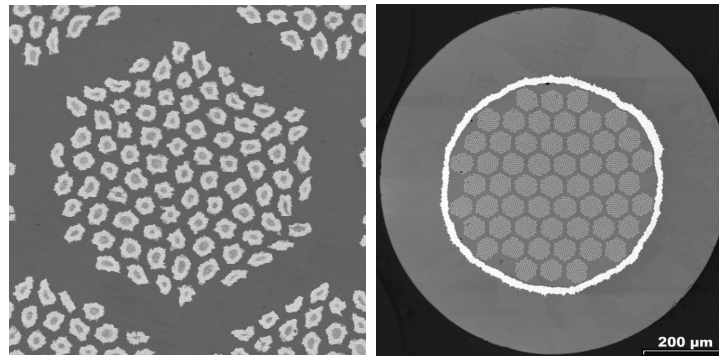


Fig. 6. EAS (European Advanced Superconductors) strand: bronze route type with filaments collected in 55 groups of 85 filaments embedded in a bronze matrix. A tantalum thick barrier divides the bronze from the outside OFE copper matrix. A detail of the SC filament group is shown on the left hand side (images: courtesy of P. Lee, University of Wisconsin – Madison Applied Superconductivity Center)

Because of its brittleness, Nb_3Sn compound cannot be extruded and drawn (as for example NbTi), but requires special manufacturing processes: a billet including uncompounded precursors of Nb_3Sn is assembled and processed until the desired wire size is obtained. The wire is then heated up to the reaction temperature (923 K for EAS strand) to allow Sn atoms to diffuse and react with Nb atoms to form Nb_3Sn precipitates. The strand is kept for several hours at high temperature because the progression rate of the reaction is rather slow. At the end it is cooled down to room temperature and then to its operating conditions (about 4.2 K).

In this work we apply the GSCL method to obtain the thermal and mechanical effective properties of the inner zone (bronze matrix and Nb_3Sn filaments) as a function of temperature, taking into account the elasto-plastic behaviour of bronze and possible filament breakage (Fig. 7). The validity of the method is tested in [37].

Two initial materials are considered: a fibrous inclusion of Nb_3Sn and a bronze matrix. We assume that the strand components are in equilibrium at 923 K without stresses and strains (the fields due

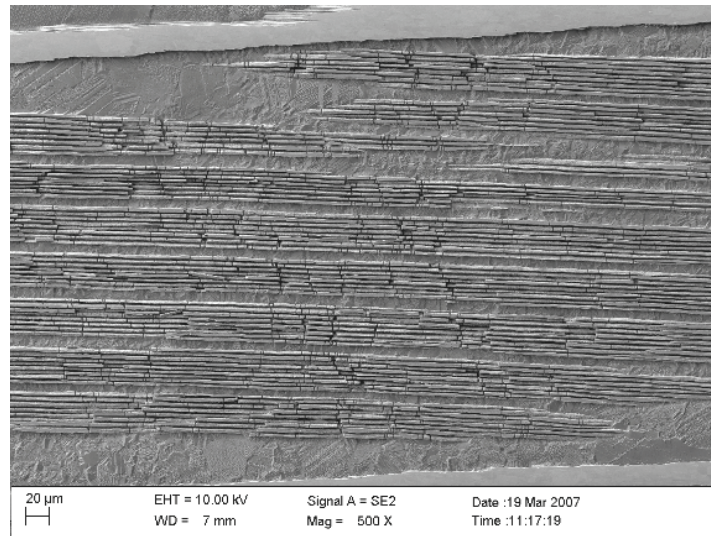


Fig. 7. SEM picture showing fracture morphology. Cracked groups of Nb_3Sn filaments are well visible (courtesy of M. Jewell)



Fig. 8. FE discretization used to solve problem 1

to the heating are relaxed since the strands remains for several hours at high temperature and at that temperature the SC compound is formed). Material characteristics are not easy to find over the whole temperature range needed, most of the data used are taken from [52].

We take into consideration a FE discretization consisting of a mesh of a certain number elements suitable to exploit the axial symmetry of our problem. In this case there are three sub-domains: Nb_3Sn , bronze and effective material (from inside to outside). The FE discretization is illustrated in Fig. 8.

In detail, three examples are shown:

- *Example A:* Elastic-plastic matrix and elastic inclusions, minimization problem solved as in Section 3.6,
- *Example B:* Elastic-plastic matrix and brittle inclusions, minimization problem solved as in Section 3.6,
- *Example C:* Elastic-plastic matrix and brittle inclusions, minimization problem solved as in Section 3.7.

4.1. Example A

The effective properties $\{E, \nu, \beta\}$ as a function of temperature, obtained with the GSCL method are presented in Figs. 9 to 11.

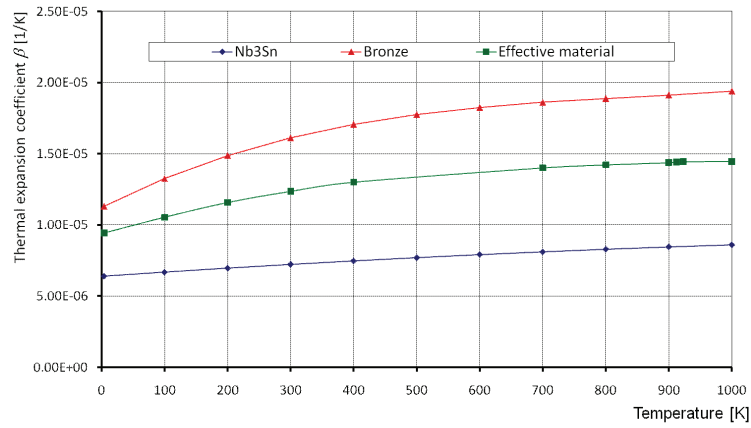


Fig. 9. Nb₃Sn, bronze and effective thermal expansion coefficient as a function of temperature

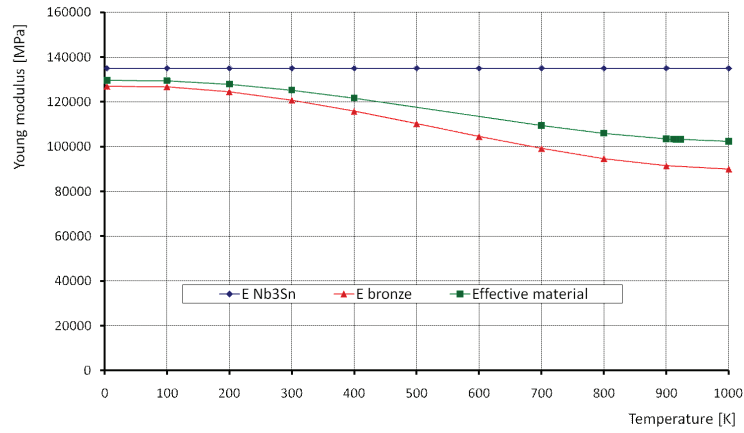


Fig. 10. Nb₃Sn, bronze and effective Young modulus as a function of temperature

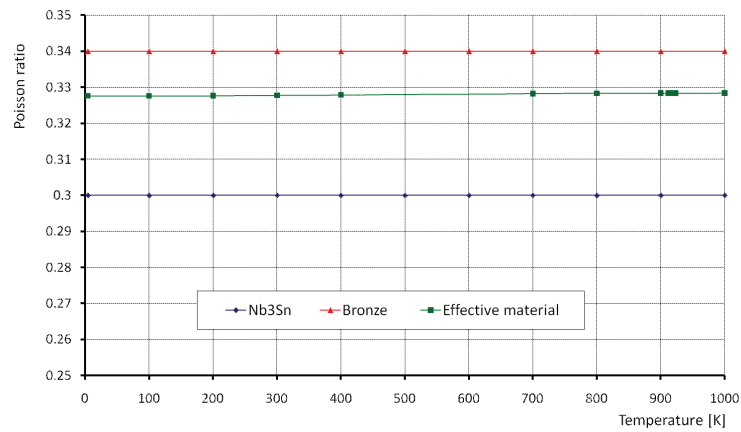


Fig. 11. Nb₃Sn, bronze and effective Poisson ratio as a function of temperature

4.2. Example B

The tests are performed for a mean distance between cracks (perpendicular to the fibres) of $50 \mu\text{m}$. This corresponds to the line AC in Fig. 2. This value is taken arbitrarily (it is one of the values occurring in Fig. 7) However, the effective material properties depend on the distance between cracks in the assumed cracking pattern. It is worth to remind that these computations are done to test the proposed method rather than to identify the real cracking phenomena. The main scope of this paper is to identify the effective material properties of the already damaged material. Namely, it is assumed that cracking occurs at 800 K first and at 600 K for a second case of analysis i.e. a simulation of a second cool down. No propagation of cracks is simulated: we consider the undamaged state and the cracked situation. On the contrary, the evolution of material yielding is taken into account: at each new temperature the new different yielded zone in the domain of bronze is calculated.

The evolution of thermal expansion coefficient and Young modulus as a function of temperature is illustrated in Figs. 12 to 14, together with the results of example A for comparison purposes.

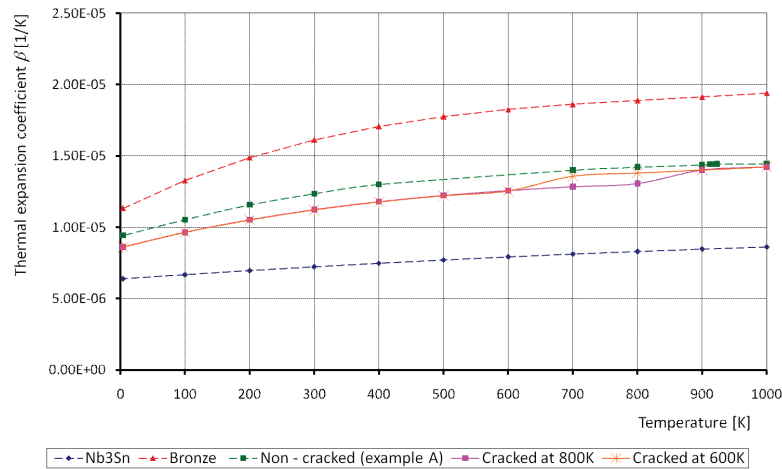


Fig. 12. Nb₃Sn, bronze and effective thermal expansion coefficient as a function of temperature. The cracking is considered once at 800 K, in a second example at 600 K

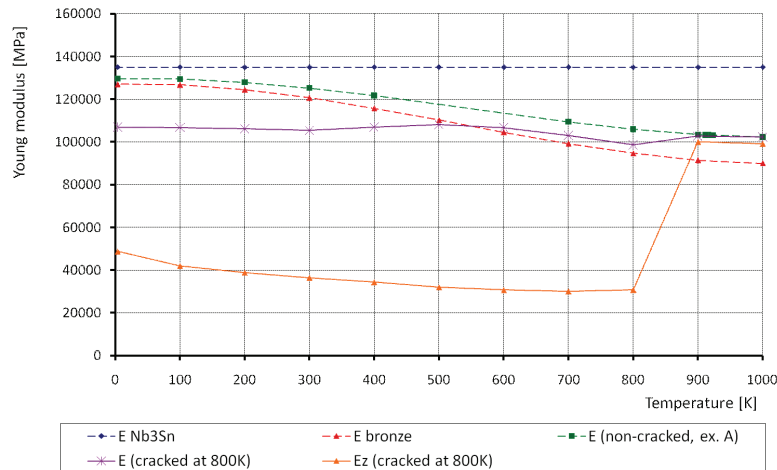


Fig. 13. Evolution of Young moduli as a function of temperature. Cracking is considered at 800 K

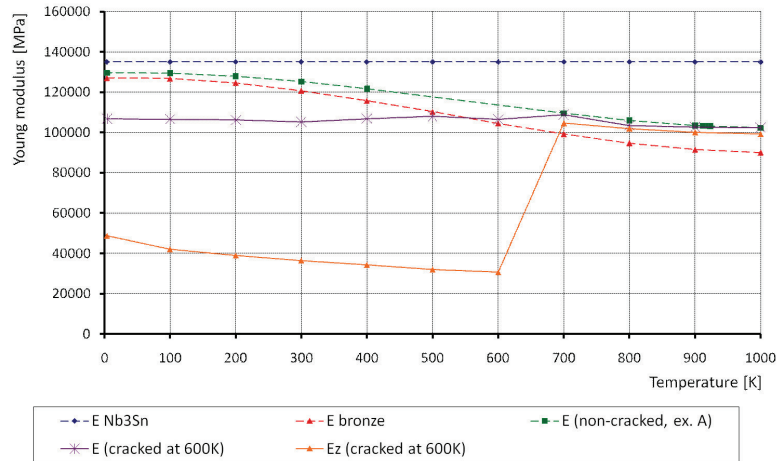


Fig. 14. Evolution of Young moduli as a function of temperature. Cracking is considered at 600 K

4.3. Example C

In this example, we have taken into consideration 11 reference temperatures and 30 training patterns at each temperature. As before, the computations are performed for a mean distance between cracks (perpendicular to the fibres) of about $50 \mu\text{m}$.

The computational approach can be summarized in three main steps:

- FE solution of the direct problem for a number of trial values of $E^{\text{eff}} = \{E, \nu, E_z, \nu_z, \beta, \beta_z\}$ and computation of the gradient \mathbf{G} ,
- training of the ANN using two vectors: gradient \mathbf{G}_i computed for trial value of $E_i^{\text{eff}} = \{E, \nu, E_z, \nu_z, \beta, \beta_z\}_i$ at the input and corresponding trial vector $E_i^{\text{eff}} = \{E, \nu, E_z, \nu_z, \beta, \beta_z\}_i$ at the output,
- computing the true effective values $E^h = \{E, \nu, E_z, \nu_z, \beta, \beta_z\}$ as a result of the ANN activity in recall mode with $\mathbf{0}$ as input vector.

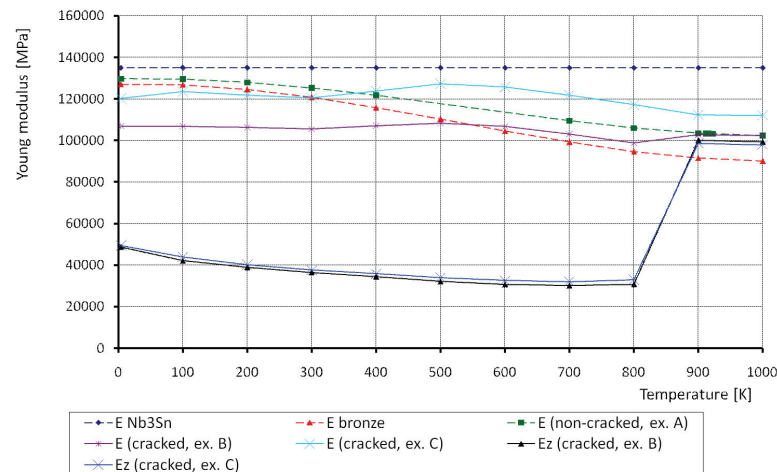


Fig. 15. Nb₃Sn, bronze and effective Young modulus as a function of temperature. The cracking is considered to take place at 800 K. The presented results are superposed with those obtained with the use of steepest gradient minimisation (examples A and B)

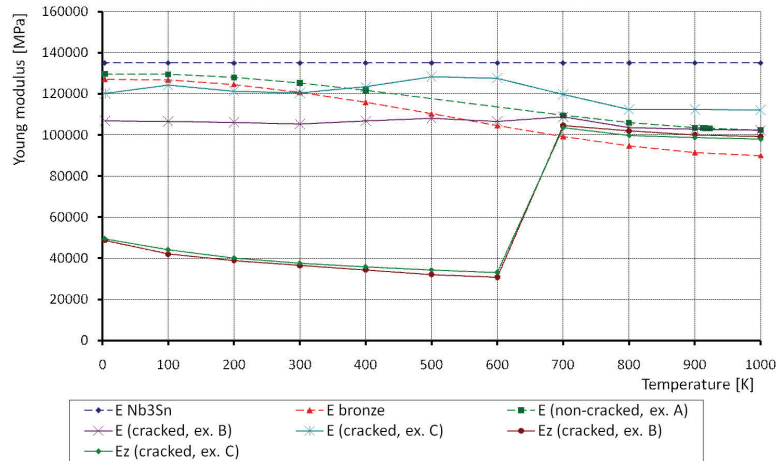


Fig. 16. Nb₃Sn, bronze and effective Young modulus as a function of temperature. The cracking is considered to take place at 600 K. The presented results are superposed with those obtained with the use of steepest gradient minimisation (examples A and B)

Figure 15 illustrates the effective Young modulus as a function of T obtained with the presented GSCL method and by supposing that superconducting filament breakage occurs at 800 K. As a matter of comparison, in the same image we presented also the effective material characteristics obtained in the previous examples. Figure 16 presents analogous results in the case that filaments break at 600 K.

5. CONCLUSIONS

The proposed method can be seen as a natural generalization of the generalized self-consistent approach. Its peculiarities consist of the possibility of taking into consideration the non linear behaviour of the initial materials, the thermo-mechanical coupling and the dependence of the properties on temperature in an efficient way.

Since the characteristics of the various phases of the composite, such as Young modulus, Poisson ratio and thermal expansion coefficient, are functions of temperature, the effective materials is also temperature dependent. The quality of the approximation of the composite behaviour by the homogenized medium depends strictly on the number and choice of the time steps and reference temperatures, but we do not need to formulate any a priori assumption on the effective behaviour. It is found as an equivalent, path-dependent “elastic” material. For the computation of effective properties, this procedure takes into account the current state of yielding of the material at the level of the microstructure and the fracture of the fibres. We have applied it to the real case of a composite superconducting strand, made of yielding bronze and brittle Nb₃Sn filaments.

Usually the self-consistent approach is associated with a symbolic expressions for the effective material parameters. On the contrary in this work we have found the solution numerically. The fully numerical approach adopted opens the ways for various experiments: minimisation of different norms of distance between thermo-mechanical behaviour of heterogeneous inclusion and a homogenized body.

We have to underline that, while the extension of the proposed algorithm of FE computations combined with the steepest gradient method seems to be easily adaptable to other kind of non-linearities (for example large deformation), a detailed formulation of the problem must be entirely redefined in that case.

We have also proposed an alternative approach for the numerical search of the effective parameters, which includes the use of artificial neural networks. It has the advantage that the number of

necessary repeated FE runs is lower. Furthermore, we observed that the algorithm of solution of the problem for the non-bijective function was active only a few times during our calculations. It means that the computational behaviour was surprisingly regular.

For the presented example (which is very difficult because of the jump of the effective properties when cracks occur), the reduction of the cost of computations was significant: it resulted about 75% lower with respect to the computations executed according to the steepest descent approach. The numerical values of the effective parameters are very close in both cases, the relative difference does not exceed 5%.

The most important disadvantage of the generalized self consistent like method is that it requires many executions of FE computations for many trial values of effective parameters describing the homogenized medium (at minimum twelve repetitions of the run of the FE code to define the gradient of the norm F_{12H}). This number is, fortunately, kept at minimum since the trial values of effective parameters are not chosen randomly. The problem of a large number of repetitions of the FE computations is reduced by the fact that the finite element mesh can be very small and quite standardized. According to our experiments, a model with about ten rectangular six node axial symmetric elements in the heterogeneous zone is accurate enough to have a good approximation of effective parameters.

On the other hand, the well known difficulties associated with the method of steepest descent are present also in the studied problem. The choice of the starting point is fundamental for the efficiency of the computation. Also the problem of the control of the speed of convergence by adaptation of the value of η at each stage of approximation is crucial. This problem has not been discussed in the paper.

In our opinion the presented preliminary results are promising since the numerical cost is reasonable and testing computations confirm the correctness and utility in engineering practice.

The best choice of the starting point, the adaptation of the rate of convergence factor and the questions related to the uniqueness of the solution are the subject of our current research.

ACKNOWLEDGEMENTS

Support for this work was partially provided by Italian Research Grant STPD08JA32_004 and Italian Research Project EX 60%—60A09-8711/09. This support is gratefully acknowledged.

We wish to thank also Eng. Yann Krysiński, for his help in the development of the FE code used in this paper.

REFERENCES

- [1] E.W.B. Engquist, X. Li, W. Ren, E. Vanden-Eijnden. Heterogeneous multiscale methods: A review. *Communications in Computational Physics*, **2**(3): 367–450, 2007.
- [2] A. Bensoussan, J.L. Lions, G. Papanicolau. *Asymptotic Analysis for Periodic Structures*. North-Holland, Amsterdam, 1976.
- [3] E. Sanchez-Palencia. *Non-Homogeneous Media and Vibration Theory*. Springer-Verlag, Berlin, 1980.
- [4] W. Voigt. Über die Beziehung zwischen den beiden Elastizitäts konstanten isotroper Körper. *Wied. Ann.*, **38**: 573–587, 1889.
- [5] A. Reuss. Berechnung der Fließgrenze von Mischkristallen auf Grund der Plastizität bedingung für Einkristalle. *Z. Angew. Math. Mech.*, **9**: 49–58, 1929.
- [6] Z. Hashin, S. Shtrikman. A variational approach to the theory of the elastic behaviour of polycrystals. *J. Mech. Phys. Solids*, **10**: 343–352, 1962.
- [7] Z. Hashin, S. Shtrikman. On some variational principles in anisotropic and nonhomogeneous elasticity. *J. Mech. Phys. Solids*, **10**: 335–342, 1962.
- [8] Z. Hashin, S. Shtrikman. A variational approach to the theory of the elastic behaviour of multiphase materials. *J. Mech. Phys. Solids*, **11**: 127–140, 1963.
- [9] D.A.G. Bruggeman. Berechnung verschiedener physikalischer Konstanten von heterogenen Substanzen. I. Dielektrizitätskonstanten und Leitfähigkeiten der Mischkörper aus isotropen Substanzen. *Ann. Phys.*, **24**: 636–679, 1935.
- [10] B. Budiansky. On the elastic moduli of some heterogeneous materials. *J. Mech. Phys. Solids*, **13**, 223–227, 1965.

- [11] A.V. Hershey. The elasticity of an isotropic aggregate of anisotropic cubic crystals. *ASME J. Appl. Mech.*, **21**, 236–240, 1954.
- [12] R. Hill. A self-consistent mechanics of composite materials. *J. Mech. Phys. Solids*, **13**: 213–222, 1965.
- [13] E. Kröner. Berechnung der elastischen Konstanten des Vielkristalls aus den Konstanten des Einkristalls. *Z. Phys.*, **151**: 504–518, 1958.
- [14] P. Suquet. Analyse limite et homogénéisation. *C. R. Acad. Sci. Paris II*, **295**: 1355–1358, 1983.
- [15] P. Suquet. Element of homogenization for inelastic solid mechanics. In: E. Sanchez-Palencia, A. Zaoui, eds., *Homogenization techniques for composite media*. Lecture Notes in Physics, **272**, pp. 193–278, Springer Verlag, New York, 1985.
- [16] G.A. Francfort. Homogenisation and Fast Oscillations in Linear Thermoelasticity. In: R.Lewis, E.Hinton, P.Betess, B.Schrefler, eds., *Numerical Methods for Transient and Coupled Problems*, pp. 382–392, Pineridge Press, Swansea, 1984.
- [17] C. Boutin. Microstructural influence on heat conduction. *Int. J. Heat Mass Transfer*, **38**(17), 3181–3195, 1995.
- [18] D.P. Boso, M. Lefik, B.A. Schrefler. Homogenisation methods for the thermo-mechanical analysis of Nb₃Sn strand. *Cryogenics*, **46**(7–8): 569–580, 2006.
- [19] D.P. Boso, M. Lefik, B.A. Schrefler. A multilevel homogenised model for superconducting strand thermomechanics. *Cryogenics*, **45**(4): 259–271, 2005.
- [20] J.F.W. Bishop, R. Hill. A theory of the plastic distortion of a polycrystalline aggregate under combined stresses. *Phil. Mag.*, **42**: 414–427, 1951.
- [21] J.F.W. Bishop, R. Hill. A theoretical derivation of the plastic properties of a polycrystalline face-center metal. *Phil. Mag.*, **42**, 1298–1307, 1951.
- [22] J.R. Willis. Variational estimates for the overall response of an inhomogeneous nonlinear dielectric. In: J.L. Ericksen, D. Kinderlehrer, R. Kohn, J.-L. Lions, eds., *Homogenization and Effective Moduli of Materials and Media*, pp. 247–263, Springer-Verlag, New York, 1986.
- [23] D.R.S. Talbot, J.R. Willis. Variational principles for inhomogeneous non-linear media. *IMA J. Appl. Math.*, **35**: 39–54, 1985.
- [24] P. Ponte Castañeda. The effective mechanical properties of nonlinear isotropic composites. *J. Mech. Phys. Solids*, **39**: 45–71, 1991.
- [25] P. Ponte Castañeda. New variational principles in plasticity and their application to composite materials. *J. Mech. Phys. Solids*, **40**: 1757–1788, 1992.
- [26] D.R.S. Talbot, J.R. Willis. Some explicit bounds for the overall behaviour of nonlinear composites. *Int. J. Solids Struct.*, **29**: 1981–1987, 1992.
- [27] Suquet, P. Overall potentials and extremal surfaces of power law or ideally plastic composites. *J. Mech. Phys. Solids*, **41**: 981–1002, 1993.
- [28] T. Olson. Improvements on a Taylor’s upper bound for rigid-plastic composites. *Mater. Sci. Eng. A*, **175**: 15–19, 1994.
- [29] J. D Eshelby. The elastic field of an ellipsoidal inclusion and related problems. *Proc. R. Soc. A*, **241**: 376–396, 1957.
- [30] T.I. Zohdi. Homogenization Methods and Multiscale Modeling. In: *Encyclopedia of Computational Mechanics. Volume 2: Solids and Structures*. John Wiley & Sons, Ltd, Chichester, 2004.
- [31] J. Aboudi. *Mechanics of Composite Materials - A Unified Micromechanical Approach*. Elsevier, Amsterdam, 1992.
- [32] R. Christensen. A critical evaluation for a class of micromechanics models. *J. Mech. Phys. Solids*, **38**(3): 379–404, 1990.
- [33] Z. Hashin. Analysis of composite materials: a survey. *ASME J. Appl. Mech.*, **50**: 481–505, 1983.
- [34] R. Hill. Continuum micromechanics of elastoplastic polycrystals. *J. Mech. Phys. Solids*, **13**: 89–101, 1965.
- [35] J.W. Hutchinson. Bounds and self-consistent estimates for creep and polycrystalline materials. *Proc. R. Soc. Lond. A.*, **348**: 101–127, 1976.
- [36] M. Berveiller, A. Zaoui. An extension of the the self-consistent scheme to plastically flowing polycrystals. *J. Mech. Phys. Solids*, **26**: 325–344, 1979.
- [37] M. Lefik, D.P. Boso, B.A. Schrefler. Generalized self-consistent homogenization using the Finite Element Method. *Z. Angew. Math. Mech.*, **89**(4): 306 – 319, 2009.
- [38] M. Lefik, D.P. Boso, B.A. Schrefler. Generalised self-consistent like method for Mechanical Degradation of fibrous composites, (submitted).
- [39] D.P. Boso, M. Lefik, B.A. Schrefler. Generalized self consistent like homogenization as an inverse problem, (submitted).
- [40] J.L. Chaboche. Continuum Damage Mechanics: Part I–General Concepts. *Journal of Applied Mechanics*, **55**: 59–64, 1988.
- [41] C. Pellegrino, U. Galvanetto, B.A. Schrefler. Numerical homogenisation of periodic composite materials with non-linear material components. *Int. J. Num. Meth. Engng.*, **46**: 1609–1637, 1999.

-
- [42] D. Boso, C. Pellegrino, U. Galvanetto, B.A. Schrefler. Macroscopic damage in periodic composite materials. *Comm. Num. Meth. Engng*, **16**(9): 615–623, 2000.
- [43] J.D. Achenbach. Quantitative nondestructive evaluation. *Int. J. Solid and Structures*, **37**(1–2): 13–27, 2000.
- [44] J.C. Simo, R.L. Taylor. A return mapping algorithm for plane stress elastoplasticity. *International Journal for Numerical Methods in Engineering*, **22**(3): 649–670, 1986.
- [45] J.C. Simo, T.J.R. Hughes. *Computational inelasticity*. Springer Verlag, 1998.
- [46] E. Hervé, A. Zaoui. Elastic behaviour of multiply coated fibre-reinforced composites. *Int. J. Engng Sci.*, **33**(10): 1419–1433, 1995.
- [47] O.C. Zienkiewicz, R.L. Taylor. *The Finite Element Method for Solid and Structural Mechanics*. Elsevier Butterworth-Hein, 2005.
- [48] L.V. Gibiansky, O. Sigmund. Multiphase composites with extremal bulk modulus. *J. Mech. Phys. Solids*, **48**: 461–498, 2000.
- [49] D.P. Boso, M. Lefik, B.A. Schrefler. Thermal and Bending Strain on Nb₃Sn Strands. *IEEE Transactions on Applied Superconductivity*, **16**(2): 1823–1827, 2006.
- [50] R. Zanino, D. P. Boso, M. Lefik, P.L. Ribani, L. Savoldi Richard, B.A. Schrefler. Analysis of Bending Effects on Performance Degradation of ITER-Relevant Nb₃Sn Strand Using the THELMA Code. *IEEE Transactions on Applied Superconductivity*, **18**(2): 1067–1071, 2008.
- [51] D.P. Boso, M.J. Lefik, B.A. Schrefler. Thermo-Mechanics of the Hierarchical Structure of ITER Superconducting Cables. *IEEE Transactions on Applied Superconductivity*, **17**(2): 1362–1365, 2007.
- [52] P. Bauer, H. Rajainmaki, and E. Salpietro. *EFDA Material Data Compilation for Superconductor Simulation*, (unpublished). EFDA CSU, Garching, April 2007.

